Supporting information

Two-Dimensional CuAg/Ti_3C_2 Catalyst for Electrochemical Synthesis of Ammonia under Ambient Conditions: a combined Experimental and Theoretical Study

Anmin Liu [a,*], Qiyue Yang [a], Xuefeng Ren [d], Mengfan Gao [a], Yanan Yang [a], Liguo Gao [a], Yanqiang Li [a], Yingyuan Zhao [e], Xingyou Liang [a], Tingli Ma [b, c, *]

[a] State Key Laboratory of Fine Chemicals, School of Chemical Engineering, Dalian University of Technology, China.

E-mail: liuanmin@dlut.edu.cn, anmin0127@163.com

[b] Department of Materials Science and Engineering, China Jiliang University, Hangzhou, 310018, China.

[c] Graduate School of Life Science and Systems Engineering, Kyushu Institute of Technology, 2-4 Hibikino, Wakamatsu, Kitakyushu, Fukuoka 808-0196, Japan.

E-mail: tinglima@life.kyutech.ac.jp

[d] School of Ocean Science and Technology, Dalian University of Technology, Panjin, 124221, China.

[e] College of Chemical Engineering and Safety, Binzhou University, Binzhou, 256603, China.

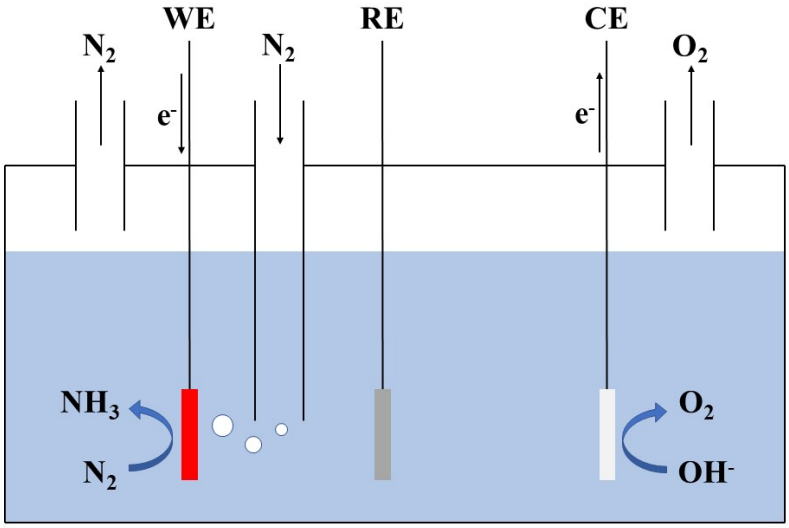

Fig. S1 Schematic diagram of the experimental cell configuration for electrocatalytic NRR

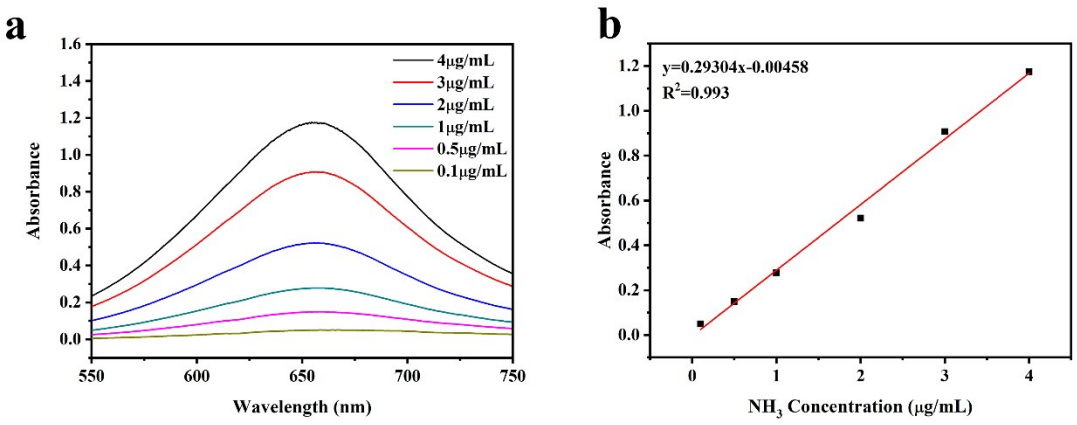

Fig. S2 UV–vis absorption spectra for standard solutions with different concentrations and calibration curve used for estimation of NH_3 concentration

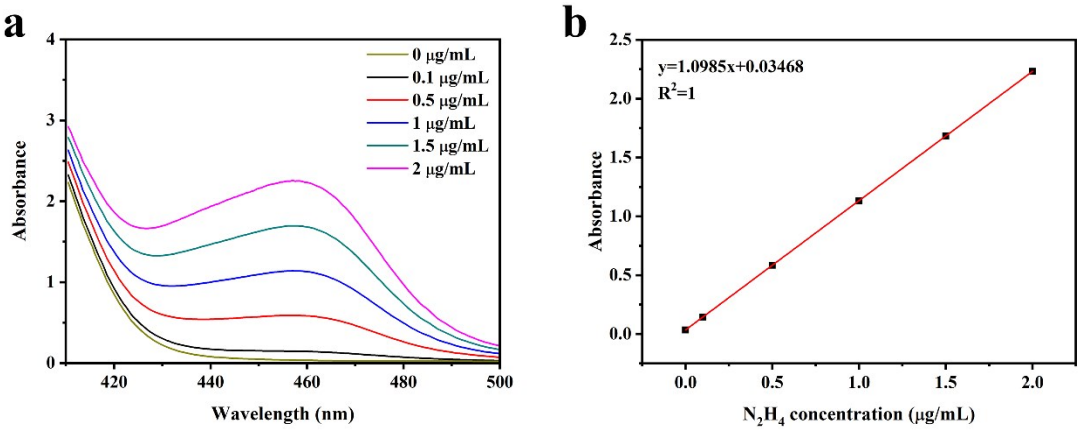

Fig. S3 UV–vis absorption spectra for standard solutions with different concentrations and calibration curve used for estimation of N_2H_4 concentration

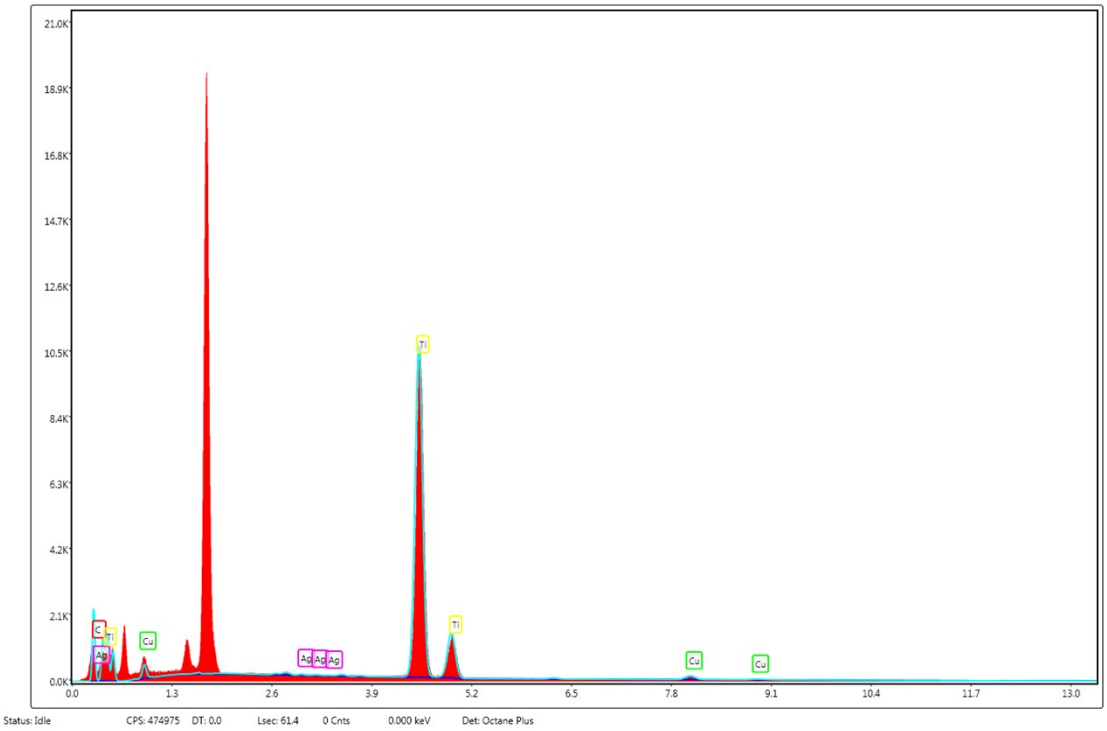

Fig. S4 EDX spectrum of $CuAg/Ti_3C_2$ (Cu:Ag = 10:1)

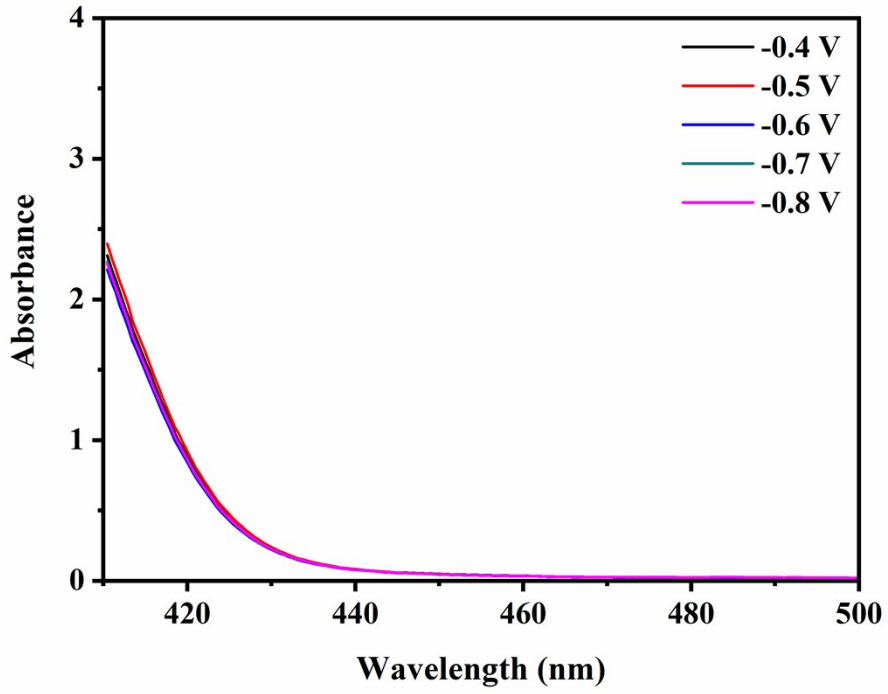

Fig. S5 UV–vis absorption spectra of 0.1 M electrolyte at different potentials

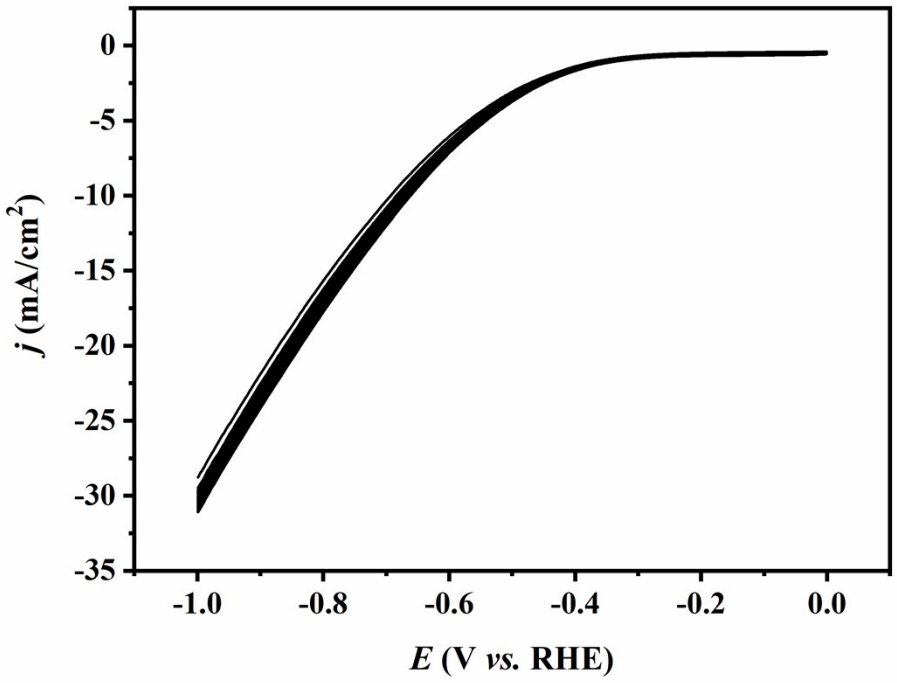

Fig. S6 CV scans of CuAg/Ti_3C_2 (Cu:Ag=10:1) for 200 cycles

Table S1. Comparison of the NRR performances for $CuAg/Ti_3C_2$ with published 2D NRR electrocatalysts.

Catalyst	Electrolyte	NH_3 yield	FE (%)	stability test	Ref.
B-doped graphene	0.05 M H_2SO_4	9.8 μg cm^{-2} h^{-1} (-0.5 V)	10.8 (-0.5 V)	5 cycles; 10 h	[1]
Bi NS	0.1 M Na_2SO_4	2.54 μg h^{-1} cm^{-2} (-0.8 V)	10.46 (-0.8 V)	6 cycles; 25 h	[2]
BNS	0.1 M Na_2SO_4	13.22 μg h^{-1} mg^{-1}_{cat} (-0.8 V)	4.04 (-0.8 V)	6 cycles; 24 h	[3]
R-WO_3 NSs	0.1 M HCl	17.28 μg h^{-1} mg^{-1}_{cat} (-0.3 V)	7.0 (-0.3 V)	6 cycles; 24 h	[4]
$Ti_3C_2T_x$	0.5 M Li_2SO_4	4.72 μg h^{-1} cm^{-2} (-0.1 V)	4.62 (-0.1 V)	6 cycles	[5]
NV-W_2N_3	0.1 M KOH	3.80×10^{-11} mol cm^{-2} s^{-1} (-0.2 V)	11.67 (-0.2 V)	12 cycles; 10 h	[6]
2DAS MoO_{3-x}	0.1 M KOH	35.83 μg h^{-1} mg^{-1}_{cat} (-0.4 V)	12.01 (-0.2 V)	16 h	[7]
MoS_2/CC	0.1 M Na_2SO_4	8.08×10^{-11} mol s^{-1} cm^{-1} (-0.5 V)	1.17 (-0.5 V)	10 cycles; 26 h	[8]
MoS_2/BCCF	0.1 M Li_2SO_4	4.38×10^{-10} mol s^{-1} cm^{-2} (-0.2 V)	9.81 (-0.2 V)	5 cycles; 12 h	[9]
TiO_2/Ti	0.1 M Na_2SO_4	9.16×10^{-11} mol s^{-1} cm^{-2} (-0.7 V)	2.50 (-0.7 V)	10 cycles; 24 h	[10]
Ru/2H-MoS_2	0.01 M HCl	1.14×10^{-10} mol s^{-1} cm^{-2} (-0.15 V, 50 ℃)	17.6 (-0.15 V, 50 ℃)	4 h	[11]
h-BNNS	0.1 M HCl	22.4 μg h^{-1} mg^{-1}_{cat} (-0.75 V)	4.7 (-0.75 V)	6 cycles; 24 h	[12]
Mn_3O_4@rGO	0.1 M Na_2SO_4	17.4 μg h^{-1} mg^{-1}_{cat} (-0.85 V)	3.52 (-0.85 V)	5 cycles; 24 h	[13]
LTO-CP	0.1 M HCl	25.15 μg h^{-1} mg^{-1}_{cat} (-0.55 V)	4.55 (-0.55 V)	6 cycles; 24 h	[14]
VN/TM	0.1 M HCl	8.40×10^{-11} mol s^{-1} cm^{-2} (-0.5 V)	2.25 (-0.5 V)	10 cycles; 8 h	[15]
$CuAg/Ti_3C_2$	0.1 M KOH	4.12 μmol cm^{-2} h^{-1} (70.04 μg cm^{-2} h^{-1}) (-0.5 V)	9.77 (-0.5 V)	5 cycles; 12 h	This work

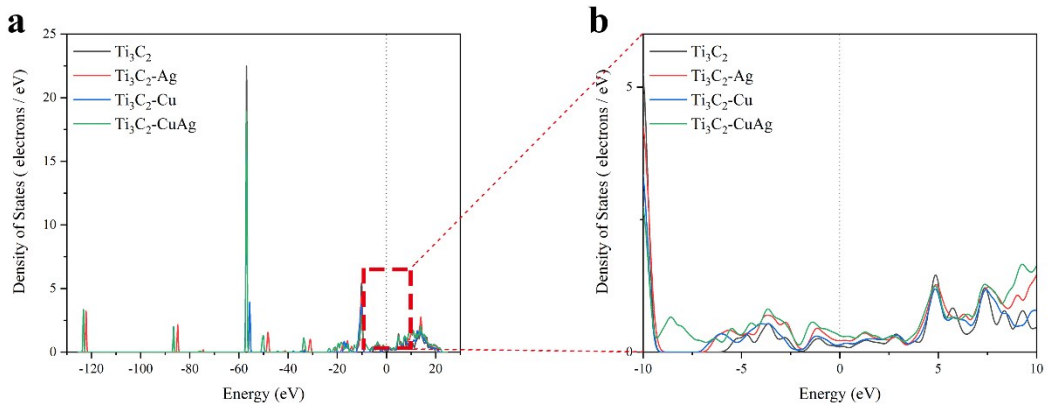

Fig. S7 s orbit PDOS of Ti_3C_2, Cu/Ti_3C_2, Ag/Ti_3C_2, and CuAg/Ti_3C_2 composite materials.

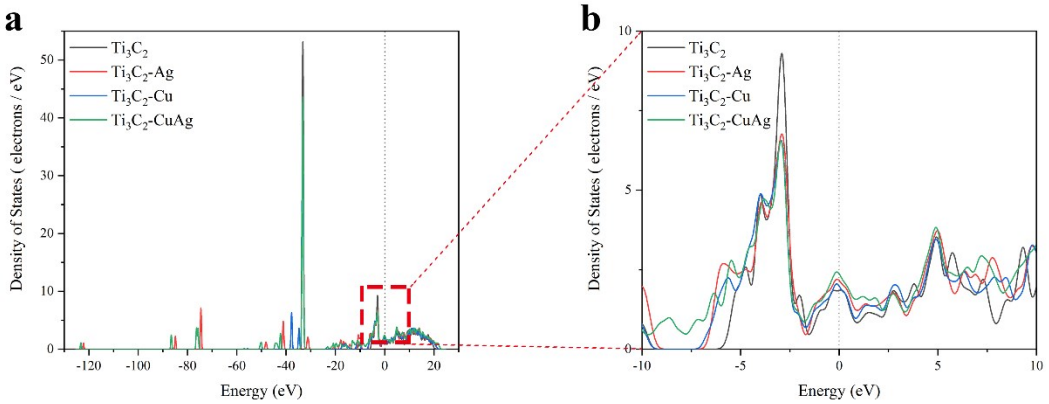

Fig. S8 p orbit PDOS of Ti_3C_2, Cu/Ti_3C_2, Ag/Ti_3C_2, and CuAg/Ti_3C_2 composite materials.

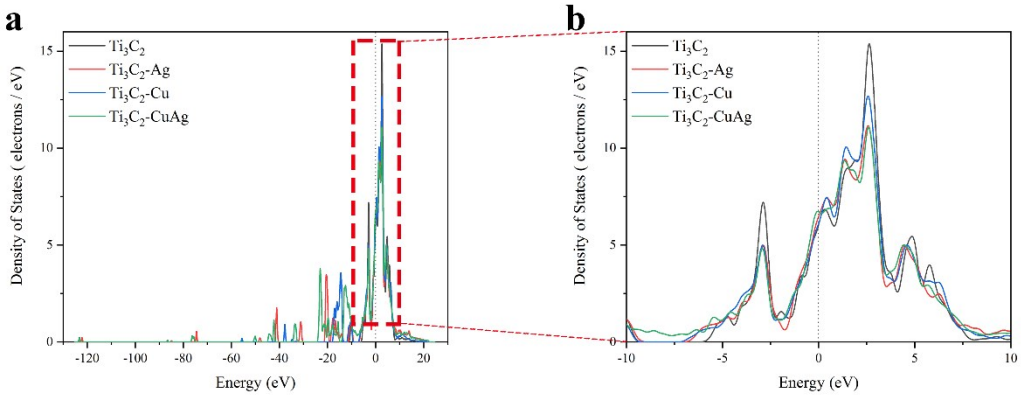

Fig. S9 d orbit PDOS of Ti_3C_2, Cu/Ti_3C_2, Ag/Ti_3C_2, and CuAg/Ti_3C_2 composite materials.

Reference

1. Yu, X.; Han, P.; Wei, Z.; Huang, L.; Gu, Z.; Peng, S.; Ma, J.; Zheng, G., Boron-Doped Graphene for Electrocatalytic N_2 Reduction. *Joule* **2018,** *2* (8), 1610-1622.

2. Li, L.; Tang, C.; Xia, B.; Jin, H.; Zheng, Y.; Qiao, S.-Z., Two-Dimensional Mosaic Bismuth Nanosheets for Highly Selective Ambient Electrocatalytic Nitrogen Reduction. *ACS Catalysis* **2019,** *9* (4), 2902-2908.

3. Zhang, X.; Wu, T.; Wang, H.; Zhao, R.; Chen, H.; Wang, T.; Wei, P.; Luo, Y.; Zhang, Y.; Sun, X., Boron Nanosheet: An Elemental Two-Dimensional (2D) Material for Ambient Electrocatalytic N_2-to-NH_3 Fixation in Neutral Media. *ACS Catalysis* **2019,** *9* (5), 4609-4615.

4. Kong, W.; Zhang, R.; Zhang, X.; Ji, L.; Yu, G.; Wang, T.; Luo, Y.; Shi, X.; Xu, Y.; Sun, X., WO_3 nanosheets rich in oxygen vacancies for enhanced electrocatalytic N_2 reduction to NH_3. *Nanoscale* **2019,** *11* (41), 19274-19277.

5. Luo, Y.; Chen, G.-F.; Ding, L.; Chen, X.; Ding, L.-X.; Wang, H., Efficient Electrocatalytic N_2 Fixation with MXene under Ambient Conditions. *Joule* **2019,** *3* (1), 279-289.

6. Jin, H.; Li, L.; Liu, X.; Tang, C.; Xu, W.; Chen, S.; Song, L.; Zheng, Y.; Qiao, S.-Z., Nitrogen Vacancies on 2D Layered W_2N_3: A Stable and Efficient Active Site for Nitrogen Reduction Reaction. *Advanced Materials* **2019,** *31* (32), 1902709.

7. Liu, W.; Li, C.; Xu, Q.; Yan, P.; Niu, C.; Shen, Y.; Yuan, P.; Jia, Y., Anderson Localization in 2D Amorphous MoO_{3-x} Monolayers for Electrochemical Ammonia Synthesis. *ChemCatChem* **2019,** *n/a* (n/a).

8. Zhang, L.; Ji, X.; Ren, X.; Ma, Y.; Shi, X.; Tian, Z.; Asiri, A. M.; Chen, L.; Tang, B.; Sun, X., Electrochemical Ammonia Synthesis via Nitrogen Reduction Reaction on a MoS_2 Catalyst: Theoretical and Experimental Studies. *Advanced Materials* **2018,** *30* (28), 1800191.

9. Liu, Y.; Han, M.; Xiong, Q.; Zhang, S.; Zhao, C.; Gong, W.; Wang, G.; Zhang, H.; Zhao, H., Dramatically Enhanced Ambient Ammonia Electrosynthesis Performance by In-Operando Created Li–S Interactions on MoS_2 Electrocatalyst. *Advanced Energy Materials* **2019,** *9* (14), 1803935.

10. Zhang, R.; Ren, X.; Shi, X. F.; Xie, F. Y.; Zheng, B. Z.; Guo, X. D.; Sun, X. P., Enabling Effective Electrocatalytic N_2 Conversion to NH_3 by the TiO_2 Nanosheets Array under Ambient Conditions. *Acs Applied Materials & Interfaces* **2018,** *10* (34), 28251-28255.

11. Suryanto, B. H. R.; Wang, D.; Azofra, L. M.; Harb, M.; Cavallo, L.; Jalili, R.; Mitchell, D. R. G.; Chatti, M.; MacFarlane, D. R., MoS_2 Polymorphic Engineering Enhances Selectivity in the Electrochemical Reduction of Nitrogen to Ammonia. *ACS Energy Letters* **2019,** *4* (2), 430-435.

12. Zhang, Y.; Du, H.; Ma, Y.; Ji, L.; Guo, H.; Tian, Z.; Chen, H.; Huang, H.; Cui, G.; Asiri, A. M.; Qu, F.; Chen, L.; Sun, X., Hexagonal boron nitride nanosheet for effective ambient N_2 fixation to NH_3. *Nano Research* **2019,** *12* (4), 919-924.

13. Huang, H.; Gong, F.; Wang, Y.; Wang, H.; Wu, X.; Lu, W.; Zhao, R.; Chen, H.; Shi, X.; Asiri, A. M.; Li, T.; Liu, Q.; Sun, X., Mn_3O_4 nanoparticles@reduced graphene oxide composite: An efficient electrocatalyst for artificial N_2 fixation to NH_3 at ambient conditions. *Nano Research* **2019,** *12* (5), 1093-1098.

14. Yu, J.; Li, C.; Li, B.; Zhu, X.; Zhang, R.; Ji, L.; Tang, D.; Asiri, A. M.; Sun, X.; Li, Q.; Liu, S.; Luo, Y., A perovskite $La_2Ti_2O_7$ nanosheet as an efficient electrocatalyst for artificial N_2 fixation to NH_3 in acidic media. *Chemical Communications* **2019,** *55* (45), 6401-6404.

15. Zhang, R.; Zhang, Y.; Ren, X.; Cui, G.; Asiri, A. M.; Zheng, B.; Sun, X., High-Efficiency Electrosynthesis of Ammonia with High Selectivity under Ambient Conditions Enabled by VN Nanosheet Array. *ACS Sustainable Chemistry & Engineering* **2018,** *6* (8), 9545-9549.